***Progress Report**:* The 3 proposals Hager submitted to SCEC were combined into one grant. As instructed by SCEC, this single report addresses the work done under all 3.

Development of Community Finite Element Models: In June, Simons and Hager ran a workshop of the Crustal Deformation Modeling (CDM) subset of the Fault Systems Working Group to begin development of community Finite Element Modeling (FEM) software. 36 scientists from 12 universities, NSF, the USGS, JPL, LANL, and GSC participated. Workshop goals were to survey what software is currently available, to define the computational challenges, and to map out a strategy for making rapid progress. FEM software can be divided into three parts: meshing, assembly of equations, and equation solving. The Workshop investigated existing codes in order to determine the relative strengths and weaknesses of academic and commercial packages. Before the Workshop, Hager and Simons designed benchmark problems to test the accuracy and efficiency of the solvers; follow on benchmarks were designed at the workshop to test the meshers. The results of this investigation (see also http://www-gpsg.mit.edu/fe) are:

***Assemblers/solvers**:* No software package identified has all the components that will be required, including efficient meshing, realistic rheologies, iterative solution of equations on distributed memory computers, and open source. Each of these is implemented in at least one available code, so could be evaluated. Benchmark comparisons were useful, demonstrating that parallel iterative solutions are both fast and accurate, but also revealing differences in physics among codes and disagreements in calculated responses that are not yet fully understood. Benchmark studies are continuing to validate codes and to assess cost vs. accuracy for various meshes.

***Meshing**:* The SCEC USR group is generating descriptions of fault geometries using triangular surfaces. A high priority emerging from the Workshop is the ability to convert the discontinuous fault segments making up CFM-A into closed surfaces bounding blocks (the Community Block Model, CBM). The most straightforward interface between USR and FEM would be achieved using tetrahedral elements; investigating the speed and accuracy of unstructured tetrahedral meshes is therefore a high priority. Given limited resources and ongoing developments by other groups, the highest priority is to develop a realistic mesh describing the fault system of southern California. We are aware of no other effort to grid such a large region with such realism. Working with Andreas Plesch and John Shaw of the USR group, we began to put together a Community Block Model (CBM) of southern CA for use in CDM studies, starting with part of the LA basin (the μCBM).

At MIT, we used the commercial finite element software Adina, which has a variety of element types and solvers, to address the cost vs. accuracy trade-off for linear and quadratic tetrahedral and hexahedral (brick) elements. We used the SCEC CDM Benchmark 4, a finite strike-slip fault in a finite domain, as our test case. Convergence tests showed that 27-node hexahedral elements are the most accurate we tested; we used the finest such mesh we could solve to define "truth." We compared accuracies of solutions on coarser grids with nodes that were a subset of those in our most accurate mesh. (Caveat: this strategy led us to use rule-based, rather than free-form tetrahedral elements.) Important results include: 1) Quadratic elements outperform linear elements in cost vs. accuracy; 2) Hexahedral elements outperform tetrahedral elements in cost vs

accuracy; 3) Relative accuracies for elastic and viscoelastic solutions are comparable; 4) Performance of linear, rule-based tetrahedral elements is unacceptable; and 5) Iterative solution via conjugate gradient has solution time increasing as the (number of nodes)$^{4/3}$, regardless of element order or shape. Former JPL/SCEC Summer Intern Teresa Baker for her MIT Senior Honors thesis is extending these tests to include free-form tetrahedral elements and test problems with variable material properties.

Inferring Fault Slip from Inversion of Geodetic Data Using Block Models*:* We divide southern California into blocks bounded by faults. A rotation about an Euler pole, with rotation vector $\mathbf{\Omega} = (\Omega_x, \Omega_y, \Omega_z)$, gives the instantaneous motion of each block. Fault slip rates, $\mathbf{v}_s$, are derived quantities, functions of the differential block velocities at a point, $\mathbf{s}(\mathbf{p}) = \mathbf{R}_s(\mathbf{p})[\mathbf{\Omega}_A - \mathbf{\Omega}_B]$, where $\mathbf{p} = (p_x, p_y, p_z)$ is position of the boundary, $\mathbf{R}_s$ is a projection matrix based on the geometry of the fault zone, and the subscripts *A* and *B* denote the blocks on either site of the fault. For any fault we allow two components of slip. Vertical faults have both strike- and tensile- slip components while all other cases have both strike- and dip-slip components. The tensile-slip component, s_t, is equal to the shortening rate, $\Delta v_\perp$, at a point. The dip slip rate, s_d, is calculated such that the component of horizontal motion is equal to the convergence rate, $s_d = \Delta v_\perp / \cos\delta$, where δ is the dip of the fault. This formulation is also sufficient to estimate block motions from geologic estimates of fault slip rates.

To relate block motions and fault slip rates to geodetic observations of secular deformation we follow the classic approach of Savage and Burford (1973). For the 2-D case, the total block velocity, $\mathbf{v}_B$, over geologic time is the sum of the interseismic, $\mathbf{v}_I$, and coseismic, $\mathbf{v}_C$, contributions. Interseismic velocity can be expressed as the difference between the block velocity, and a coseismic slip deficit (aka backslip), $\mathbf{v}_I = \mathbf{v}_B - \mathbf{v}_C$. We extend this approach to 3-D using fault segments defined by block boundaries. The block motion contribution to the interseismic velocity field is given by $\mathbf{v}_B = \mathbf{\Omega} \times \mathbf{p} = \mathbf{R}_B \mathbf{\Omega}$.

To calculate the coseismic slip deficit contribution to the velocity field we use Greens functions for the surface deformation due to a dislocation in a uniform elastic half space (Okada, 1985). We project the fault geometry and station positions from spherical to Cartesian geometry. While the distortion due to projection over an area the size of southern California is not large (< 5%) the desire to incorporate far field velocities (e.g. in the middle of the Pacific and North American plates) have motivated us to take use multiple projections. Every fault segment is divided into small pieces ≤ 10 km long; for each segment we model accurately the elastic deformation in the immediate vicinity of the fault where the velocity gradients are largest. We use a local projection for each fault segment, compute the elastic contribution and then rotate all the velocities back into an east, north, up frame. A locally tangent oblique Mercator projection allows us to flatten the geometry such that the fault trace is approximated as a great circle path between its two endpoints. The elastic (or coseismic slip deficit) contribution to the velocity field can be written as, $\mathbf{v}_C = \mathbf{R}_p(\mathbf{p})\mathbf{s}$, where $\mathbf{R}_p(\mathbf{p})$ is a projection matrix. Note that the elastic contribution is linear in slip rate and can therefore be written in terms of the rotation vectors. We can write the interseismic deformation in terms of the rotation vectors as $\mathbf{v}_I = \mathbf{R}(\mathbf{p})\mathbf{\Omega}$.

In the last year we have accomplished our goal of producing a block model of Southern California. After working with a heavily modified version of Souter's (1998) block modeling code, we decided that our present needs and future goals demanded new software built from the ground up. One year and 40,000 lines of code later we have a powerful tool (blocks_sp1) that fulfills our needs. Highlights include a natural longitude and latitude coordinate system at the user level, a point and click interface for creating and modifying fault system geometry, and the ability to include GPS velocities, fault slip rates, and Euler poles into a single inversion.

The SCEC3.0 Crustal Motion Model is a product of judicious editing. Only about a third of the more than 1500 unique station positions in southern California are included in the final product. The 1992 Landers earthquake interrupts some of the longer station time series and is the source of most challenges. For many stations installed after Landers, rapid postseismic deformation signals are evident for at least two years following the event. Many other stations have been eliminated on the basis of large deviation from neighboring stations and disagreement with the block model.

We investigated a vast suite of models for southern California that differed in the number of blocks and the geometry of the fault system. Our preferred model has relatively few (15) blocks, yet includes many important details of the fault geometry, especially in the Transverse Ranges. Using the preliminary SCEC3.0 velocity field we estimated slip rates on our model faults. The strike slip rates are shown in Fig.1. The model has 32 ± 1 mm/yr right lateral slip on the San Andreas north of the Carrizo Plain. Through the Big Bend, the Mojave and San Bernadino segments of the SAF (SBSAF) move at 22 ± 2 and 3 ± 2 mm/yr respectively. The latter rate is surprising but is a natural consequence of the fault system geometry. The SBSAF is caught between the Eastern California Shear Zone (ECSZ) carrying about 14 mm/yr and the San Jacinto Fault (SJF) to the west with 22 mm/yr, leaving little motion to be accommodated across the SBSAF itself. The faults from the Cucamonga to the San Cayetano fault accommodate the majority of the shortening in the Transverse ranges (5-8 ± 2 mm/yr of dip slip). With the exception of the Cucamonga fault, the same set of faults also has about 5 mm/yr of left lateral motion. The strand of faults (Raymond Hills to the Santa Monica Mountains fault) to the south shows < 3mm/yr motion.

GPS slip inversions: Layered (1D) elastic Earth structure and postseismic deformation

Post-doc Elizabeth Hearn characterized how elastic layering of the lithosphere affects surface deformation from strike-slip dislocations in the upper crust relative to deformation in an elastically uniform Earth (Hearn, E. H., *Bull. Seismo. Soc. Am.,* in preparation, 2002). The point of this work was to quantify how fault slip estimates from GPS and inSAR data, which typically assume the Earth is an elastic halfspace, underestimate the depth and magnitude of earthquake slip, and magnitudes of coseismic stresses. Our approach was to forward model surface displacements due to slip in an elastically layered Earth, then to invert these displacements for slip with an inversion code based on analytical solutions for a dislocation in an elastic halfspace (Okada, 1985). We forward model displacements resulting from three earthquakes with rupture dimensions of 32x16, 64x16, and 64x24 km, and three meters of slip. We examine four three-layer elastic models, as well as a uniform reference model (for benchmarking our FE-modeled displacements against analytic ones).

If GPS sites are equally spaced and located within 60 km of the fault, a shear modulus contrast of 2 at the mantle has little effect on the estimated slip relative to a uniform-elasticity model. As the rigidity of the lower crust (16-32 km depth) is increased, however, uniform-elasticity slip inversions begin to significantly underestimate both seismic moment and centroid depth relative to the forward modeled slip. For example, given a 33% increase in shear modulus, G, at 16 km depth, uniform-elasticity inversions underestimate moment and centroid depth by 20 and 30-40%, respectively. For a broader network of equally spaced GPS sites within 90 km of the fault, the uniform-elasticity inversion method underestimates seismic moment and shear modulus by 10-20% and 50-60%, respectively, if G doubles at 32 km depth. Adding a 33% increase in G at a depth of 16 km, uniform-elasticity inversions of displacements from the broader network underestimate moment and centroid depth by 15 to 30% and 50 to 60%, respectively. This brings us to a quandary: although sites far (i.e., 40 to 80 km) from the rupture are required to constrain deep slip, displacements at these sites are affected more by elastic layering than sites close to the rupture, and including them in Okada slip inversions results in errors. If only displacements close to the rupture are available (as for a typical interferogram), Okada and layered-Earth inversions yield similar results, though the resolution of slip deep on the fault is poor in both cases. Sites beyond about 80 km from the rupture contribute little to our earthquake slip estimates because of small displacements (and small differences between different modeled displacements) relative to our assumed measurement errors (2 and 10 mm for horizontal and vertical components, respectively).

Hearn also explored time-dependent surface deformation due to different postseismic deformation processes, i.e, afterslip and relaxation of horizontal viscoelastic layers (Hearn, E. H., What can GPS data tell us about the dynamics of postseismic displacements? *GJI*, submitted, 2002). We modeled surface deformation following a Mw7.4 strike-slip earthquake due to afterslip (stable frictional slip or viscous shear zone creep) and viscoelastic relaxation of layers of varying thickness and depth, and stress exponent (1 and 3). Our goal was to determine whether current GPS measurements are sufficiently precise to identify the cause of postseismic deformation, or at least to rule out certain classes of models. We found that early after an earthquake, deformation due to relaxation of a viscoelastic layer depends on both the layer thickness and viscosity (not just the Elsasser time), thus, both of these quantities may be independently estimated from surface deformation. Although complex time-dependence of deformation complicates analysis of the data, it provides us with a powerful tool for ruling out many classes of non-unique viscoelastic relaxation models. Surface deformation due to afterslip, on the other hand, does not tend to vary as much over time. We conclude that GPS is sufficiently precise to distinguish between different postseismic deformation processes if networks include frequently-monitored sites far from the fault and along strike beyond the rupture tip.

Using 3-D viscoelastic FEM, grad student Eric Hetland (Hetland, E. A. and B. H. Hager, Postseismic relaxation across the Central Nevada Seismic belt, *J. Geophys. Res.,* submitted, 2002) investigated models of ongoing postseismic deformation in Nevada following the the 1915 Pleasant Valley event (M_0=2.0 10^{20} Nm), the 1954 Fairview Peak event (M_0=0.8 10^{20} Nm), and the 1954 Dixie Valley event (M_0=0.6 10^{20} Nm). For plausible viscoelastic structures (e.g., a 15-km thick viscoelastic lower crust with Maxwell time

= 10 yrs), the sum for the 3 events shows > ± 3 mm/yr variation in E-W velocity associated with ongoing postseismic deformation. This ongoing viscoelastic relaxation provides a satisfying explanation for the otherwise anomalous compression observed in GPS velocities between eastern and Central NV.

Seismicity simulator: Hager is involved in the workshop of the Fault Systems Group that will be held in December at Davis. The goal is to facilitate the development of a SCEC seismicity simulator. The workshop will address such issues as geometry, boundary conditions, and geodetic constraints, with an emphasis on establishing as much commonality as is feasible between CDM models and seismicity simulators.

Education and Outreach*:* This grant provided partial support for Dr. Elizabeth Hearn, a young woman scientist who has now accepted a faculty position at the University of British Columbia. Ms. Teresa Baker, a young woman who was introduced to Earthquake Science through the SCEC Intern Program, is working on this project for her senior honors thesis. We also hired a high school junior for the summer, Mr. Kimon Ionnaides of Concord Academy, who contributed to this project by improving the performance of our PC cluster (which was purchased by MIT as part of its SCEC cost match); we contributed to his education by engaging him in our research group. As a result, he considers scientific research to be his likely career path. Finally, this grant supported the education of two graduate students, Eric Hetland and Brendan Meade.

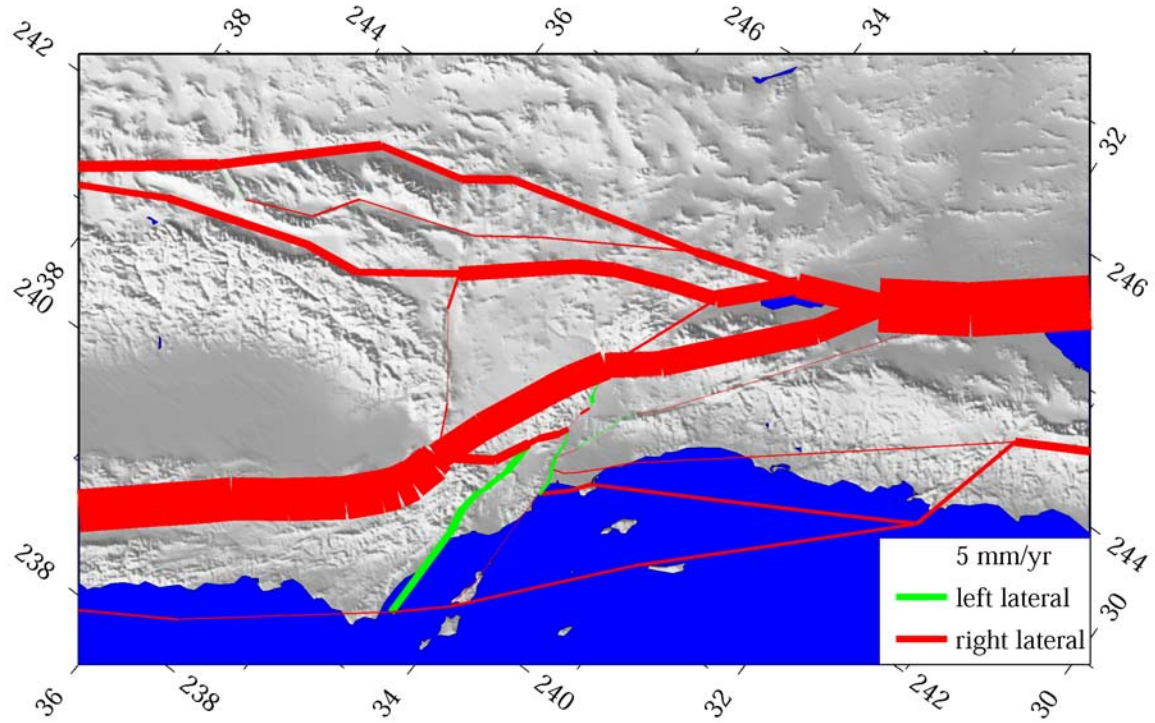

Figure 1: The strike slip rates estimated from our block model are shown in an oblique projection of southern California, where north is toward the upper left corner. The width of the lines is proportional to the fault slip rate with red and green indicating right and left lateral motion respectively.